Genuinely noncyclic geometric gates in two-pulse schemes

Nils Eivarsson and Erik Sjöqvist[*]

Department of Physics and Astronomy, Uppsala University, Box 516, Se-751 20 Uppsala, Sweden

While most approaches to geometric quantum computation are based on geometric phases in cyclic evolution, noncyclic geometric gates have been proposed to increase further the flexibility. While these gates remove the dynamical phase of the computational basis, they do not, in general, remove it from the eigenstates of the time evolution operator, which makes the geometric nature of the gates ambiguous. Here, we resolve this ambiguity by proposing a scheme for *genuinely noncyclic geometric gates*. These gates are obtained by evolving the computational basis along open paths consisting of geodesic segments, and simultaneously assuring that no dynamical phase is acquired by the eigenstates of the time evolution operator. While we illustrate the scheme for the simplest nontrivial case of two geodesic segments starting at each computational basis state of a single qubit, the scheme can be straightforwardly extended to more elaborate paths, more qubits, or even qudits.

I. INTRODUCTION

Quantum computation is a form of information processing that uses quantum mechanical properties, such as superposition and entanglement, to perform calculations. Although quantum computers of today do not have the number of qubits required for realizing programmable large-scale computation, progress towards this goal has been achieved [1] on different experimental platforms [2–4].

It is not, however, enough to scale up quantum computers; they also need to be resilient to noise and decoherence under which qubits would lose their desired quantum mechanical properties. The state within a quantum computer cannot be completely isolated and decoherence is therefore inevitable. It is possible to overcome this problem according to the threshold theorem [5,6], which entails that an arbitrarily long quantum computation can be sustained by error correction techniques provided the error rate per gate is below a certain threshold value.

One approach to reach below this threshold is to use geometric quantum gates [7–13]. These are based on the (Abelian) geometric phase (GP) of quantum systems [14,15]. When a quantum state undergoes a cyclic evolution it can gain a phase factor. This phase factor can be split into a dynamical part and a geometric part, where the geometric part is only dependent on the path a quantum state takes through its state space. By choosing an evolution for which the dynamical phase effect is trivial, it is possible to implement quantum logic gates that are purely dependent on the geometry of the path. This dependency on only geometry can be shown to be resilient against certain types of noise [16–23].

While geometric quantum gates show promise in the implementation of robust quantum computers, there are still improvements to be made before they are fully operational. One possible improvement is to reduce the number of pulses and the run time needed to implement the gates, as this would reduce the qubits' exposure to the environment, thereby limiting the effect of decoherence, as well as simplifying the pulse schemes. To reduce the run time, noncyclic evolution in the implementation of geometric quantum gates have been proposed [24–31] and experimentally implemented [32]. These gate are based on computational states evolving along open paths while still only acquiring a GP in noncyclic evolution [33,34]. However, while the GP factors acquired by the computational states are eigenvalues of the time evolution operator when implementing cyclic geometric gates, this is not so in noncyclic evolution since, in this case, the eigenstates do not coincide with the computational states. This means that the eigenstates may pick up additional nontrivial dynamical phases also in cases where the noncyclic gates look geometric in the computational basis. Thus, the geometric meaning of these noncyclic gates is ambiguous.

Here, we propose precise conditions for geometric gates. Under these conditions the meaning of noncyclic geometric gates become unambiguous. This provides a notion of *genuinely noncyclic geometric gates*. Furthermore, geometric gates under cyclic evolution of the computational states, which are gates that trivially satisfy these conditions, are Abelian (they diagonalize in the computational basis) and therefore fail universality. To complete the universal set, we shall thus see that at least one genuinely noncyclic geometric gate is needed.

*erik.sjoqvist@physics.uu.se

II. CONDITIONS FOR GEOMETRIC GATES

We consider Schrödinger evolution $i\hbar|\dot{\psi}(t)\rangle = H(t)|\psi(t)\rangle$, where $H(t)$ is the Hamiltonian of the system

with Hilbert space $\mathcal{H}$. Let $U(t,0) = \mathbf{T}e^{-\frac{i}{\hbar}\int_0^t H(t')dt'}$ be the corresponding time evolution operator. We assume that the computational system consists of n qubits with state space $\mathcal{M} \subseteq \mathcal{H}$ spanned by $2^n \leqslant \dim \mathcal{H}$ predetermined computational state vectors $\{|\vec{q}\rangle = |q_1, \ldots, q_n\rangle\}_{q_1,\ldots,q_n=0,1}$, fixed by the final readout of the computation.

Let $U(\tau, 0)$ be the desired gate realized during the time interval $t \in [0, \tau]$. Consider the eigenvalue equation

$$U(\tau, 0)|\psi_k\rangle = e^{i\varphi_k}|\psi_k\rangle, \quad k = 1, \ldots, 2^n. \tag{1}$$

Here, $\{|\psi_k\rangle\}$ is an orthonormal set of vectors since $U(\tau, 0)$ is a normal operator [5]. We assume that $U(\tau, 0)$ preserves $\mathcal{M}$, i.e., $|\psi_k\rangle = \sum_{\vec{q}} c_{\vec{q}}^{(k)}|\vec{q}\rangle$, $\forall k$, even in the case where $2^n < \dim \mathcal{H}$. Thus, $U(\tau, 0)U^\dagger(\tau, 0)$ is a projection operator on $\mathcal{M}$.

The action of $U(\tau, 0)$ on each computational state $|\vec{q}\rangle$ can be understood in terms of its GP

$$\Gamma_{\vec{q}} = \arg\langle\vec{q}|U(\tau, 0)|\vec{q}\rangle + i \int_0^\tau \langle\vec{q}|U^\dagger(t, 0)\dot{U}(t, 0)|\vec{q}\rangle dt, \tag{2}$$

provided $\langle\vec{q}|U(\tau, 0)|\vec{q}\rangle$ is nonzero. $\Gamma_{\vec{q}}$ is real-valued and a property of the path $U(t, 0)|\vec{q}\rangle\langle\vec{q}|U^\dagger(t, 0)$ in state space, as it is invariant under monotonic reparametrizations $t \mapsto s(t)$ and time-local phase changes $U(t, 0) \mapsto e^{if(t)}U(t, 0)$ [34]. These $\Gamma_{\vec{q}}$:s are generically noncyclic GPs as the paths in state space are typically open. On the other hand, the eigenvectors $|\psi_k\rangle$ of $U(\tau, 0)$ are the cyclic states of the evolution $U(t, 0)$, $t \in [0, \tau]$, and may thus be analyzed by using the Aharonov-Anandan GP [15]. In this framework, each cyclic phase φ_k contains a geometric (γ_k) and a dynamical (δ_k) part, given by

$$\gamma_k = \arg\langle\psi_k|U(\tau, 0)|\psi_k\rangle + i \int_0^\tau \langle\psi_k|U^\dagger(t, 0)\dot{U}(t, 0)|\psi_k\rangle dt, \tag{3}$$

and

$$\delta_k = -\frac{1}{\hbar}\int_0^\tau \langle\psi_k|U^\dagger(t, 0)H(t)U(t, 0)|\psi_k\rangle dt, \tag{4}$$

such that $\varphi_k = \gamma_k + \delta_k$.

Based on the above, we can now define a *genuinely noncyclic geometric gate* (GNGG) as a unitary $U(\tau, 0)$ that satisfies the following two conditions:

(i) $\Gamma_{\vec{q}} - \Gamma_{\vec{0}} = \arg\langle\vec{q}|U(\tau, 0)|\vec{q}\rangle - \arg\langle\vec{0}|U(\tau, 0)|\vec{0}\rangle$, mod 2π,

(ii) $\delta_k - \delta_1 = 0$, mod 2π,

for all k and binary vectors $\vec{q}$. In essence, such a gate depends only on GPs for both its eigenstates and the predetermined computational states.

Before addressing the physical realization of GNGGs in the next section, we consider some qubit gates assuming them to be genuinely noncyclic to gain some further conceptual insights. First, let us consider a genuinely noncyclic geometric Hadamard gate $\mathbb{H}$. Such a gate takes the form

$$\mathbb{H} = \frac{1}{\sqrt{2}}(|0\rangle + |1\rangle)\langle0| + e^{i\pi}\frac{1}{\sqrt{2}}(|1\rangle - |0\rangle)\langle1| \tag{5}$$

in the computational basis [35,36], and

$$\mathbb{H} = |+\rangle\langle+| + e^{i\pi}|-\rangle\langle-| \tag{6}$$

in the eigenbasis $|\pm\rangle = \frac{1}{4 \mp 2\sqrt{2}}[|0\rangle - (1 \mp \sqrt{2})|1\rangle]$, with the phase factor $e^{i\pi} = -1$ assumed to be geometric in both cases. We thus see that the geometric phase difference for both forms is π, i.e., $\Gamma_1 - \Gamma_0 = \gamma_2 - \gamma_1 = \pi$.

As a second example, we consider rotation gates $\mathbb{U}_z(\vartheta_z) = e^{-i\frac{\vartheta_z}{2}\sigma_z}$ and $\mathbb{U}_y(\vartheta_y) = e^{-i\frac{\vartheta_y}{2}\sigma_y}$ that can be used to describe an arbitrary single-qubit rotation [37]. First, we note that $\mathbb{U}_z(\vartheta_z)$ is diagonal in the computational basis, i.e., the eigenbasis coincides with the computational basis. This implies that the gate is a standard cyclic geometric gate [8], for which $\Gamma_1 - \Gamma_0 = \gamma_2 - \gamma_1 = \vartheta_z$. More interesting is the genuinely noncyclic geometric implementation of $\mathbb{U}_y(\vartheta_y)$. We may write

$$\mathbb{U}_y = \left(\cos\frac{\vartheta_y}{2}|0\rangle + \sin\frac{\vartheta_y}{2}|1\rangle\right)\langle0|$$
$$+ \left(-\sin\frac{\vartheta_y}{2}|0\rangle + \cos\frac{\vartheta_y}{2}|1\rangle\right)\langle1| \tag{7}$$

and

$$\mathbb{U}_y = e^{-i\frac{\vartheta_y}{2}}|y_+\rangle\langle y_+| + e^{i\frac{\vartheta_y}{2}}|y_-\rangle\langle y_-|,$$
$$|y_\pm\rangle = \frac{1}{\sqrt{2}}(|0\rangle \pm i|1\rangle) \tag{8}$$

in the computational basis and eigenbasis, respectively. Provided $\vartheta_y \neq \pi$, we find $\Gamma_1 - \Gamma_0 = 0$ and $\gamma_2 - \gamma_1 = \vartheta_y$, i.e., while the noncyclic GP difference of the computational basis states is trivial, the cyclic GP difference is generally not. In the case where $\vartheta_y = \pi$, the noncyclic phases are not defined as the computational states are each mapped on orthogonal states. It follows, more generally, that π rotations around any axis in the xy plane cannot be implemented in a genuinely noncyclic manner. Curiously, this implies that there is no genuinely noncyclic implementation of CNOT, while the GNGG scheme can be used to realize other entangling two-qubit control gates with noncyclic and cyclic GPs 0, 0, Γ_{10}, Γ_{11} and 0, 0, γ_3, γ_4, respectively. Similarly, the SWAP gate cannot be implemented as a GNGG since it interchanges the computational states $|01\rangle$ and $|10\rangle$, which are orthogonal in both qubits, while a genuinely noncyclic realization of the $\sqrt{\text{SWAP}}$ gate exists. The latter takes the form

$$\sqrt{\text{SWAP}} = |00\rangle\langle00| + e^{i\frac{\pi}{4}}\frac{1}{\sqrt{2}}(|01\rangle - i|10\rangle)\langle01|$$
$$+ e^{i\frac{\pi}{4}}\frac{1}{\sqrt{2}}(-i|01\rangle + |10\rangle)\langle10| + |11\rangle\langle11| \tag{9}$$

in the computational basis and

$$\sqrt{\text{SWAP}} = |e_1\rangle\langle e_1| + |e_2\rangle\langle e_2| + e^{i\frac{\pi}{2}}|e_3\rangle\langle e_3| + |e_4\rangle\langle e_4| \tag{10}$$

in the eigenbasis $|e_1\rangle = |00\rangle$, $|e_2\rangle = \frac{1}{\sqrt{2}}(|01\rangle + |10\rangle)$, $|e_3\rangle = \frac{1}{\sqrt{2}}(|01\rangle - |10\rangle)$, $|e_4\rangle = |11\rangle$. One finds the noncyclic and cyclic GPs $\Gamma_{00} = \Gamma_{11} = 0$, $\Gamma_{01} = \Gamma_{10} = \frac{\pi}{4}$ and $\gamma_1 = \gamma_2 = \gamma_4 = 0$, $\gamma_3 = \frac{\pi}{2}$, respectively. Both these sets define nontrivial GP differences.

III. TWO-PULSE SINGLE-QUBIT GATES

A key point of the GNGG technique is that it can be used to reduce the number of pulses to implement a universal set of geometric gates. To make this point explicit, we shall now examine the physical realization of arbitrary genuinely non-cyclic single-qubit gates by using the simplest nontrivial case of two pulses. To achieve universality with geometric gates in such schemes, adhering to the proposed conditions (i) and (ii) above, noncyclic geometric gates are required, as cyclic gates are inherently Abelian in that they are by definition diagonal in the computational basis and thus insufficient for universality [38].

Let the two pulses be applied during $[0, t_1]$ and $[t_1, \tau]$, respectively. By choosing the pulses such that they move the computational basis along a pair of geodesic segments, the corresponding dynamical phases vanish. After constructing these gates, the dynamical phases of the eigenstates of the time evolution operator are studied to find which gates are genuinely geometric, i.e., satisfy the condition $2\delta = 0$, mod 2π, where we use that $\delta_0 = -\delta_1 \equiv \delta$. As we shall see, this requires a careful tuning of rotation axes and precession angles associated with the two pulses.

A path is geodesic on the Bloch sphere when the axis $\mathbf{n}$ of rotation is orthogonal to the initial Bloch vector. Since the first pulse acts on the computational basis $\{|q\rangle\}_{q=0,1}$, it should thus correspond to a rotation around any axis $\mathbf{n}_1$ in the xy plane, as this would result in evolution of these states along parts of a great circle that pass through the poles of the Bloch sphere. Choosing one axis over another only changes the eigenvector of the complete evolution by a rotation around the z axis. We can therefore limit ourselves to one specific axis of rotation and later generalize to other axes in the xy plane by simply rotating the gate. We choose the y axis, i.e., $\mathbf{n}_1 = \mathbf{e}_y$, which defines the Hamiltonian

$$H_1 = \tfrac{1}{2}\hbar\omega\,\sigma_y, \qquad (11)$$

with corresponding time evolution operator

$$U_1(t,0) = e^{-\frac{i}{2}\omega t}|y_+\rangle\langle y_+| + e^{\frac{i}{2}\omega t}|y_-\rangle\langle y_-|. \qquad (12)$$

At the final time t_1 of the first pulse, the qubit has rotated an angle $\theta_1 = \omega t_1$. This rotation can be seen in the upper panel of Fig. 1.

For the second pulse, the axis of rotation must be orthogonal to the final state of the first pulse to move the qubit state along a geodesic. Starting at $|0\rangle$, the final state of the first pulse can be described by the Bloch vector $\mathbf{r}_1 = \sin\theta_1\mathbf{e}_x + \cos\theta_1\mathbf{e}_z$, which serves as initial state for the second pulse. The axis of rotation can therefore be taken as

$$\mathbf{n}_2 = -\cos\theta_1\cos\phi\,\mathbf{e}_x + \sin\phi\,\mathbf{e}_y + \sin\theta_1\cos\phi\,\mathbf{e}_z. \quad (13)$$

This lies in the plane spanned by the vector $-\cos\theta_1\,\mathbf{e}_x + \sin\theta_1\,\mathbf{e}_z$, orthogonal to $\mathbf{r}_1$, and the y axis. ϕ is the rotational angle around $\mathbf{r}_1$ relative to the xz plane, see the lower panel of Fig. 1. With the axis of rotation defined, the Hamiltonian becomes

$$H_2 = \frac{\hbar\omega}{2}(-\cos\theta_1\cos\phi\,\sigma_x + \sin\phi\,\sigma_y$$
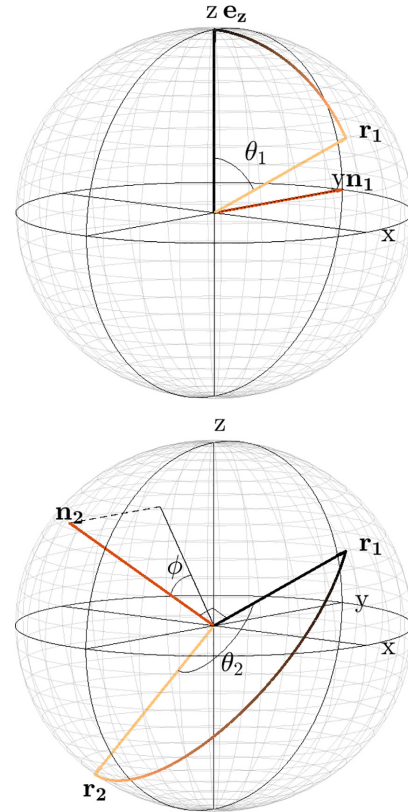$$+ \sin\theta_1\cos\phi\,\sigma_z), \qquad (14)$$

FIG. 1. The rotation of the qubit during the first pulse (upper panel). θ_1 is the rotational angle and $\mathbf{n}_1$ is the axis of rotation. The rotation of the qubit during the second pulse (lower panel). θ_2 is the rotational angle and ϕ determines the axis of rotation $\mathbf{n}_2$. $\mathbf{n}_2$ is orthogonal to the final state (with Bloch vector $\mathbf{r}_1$) of the first pulse. The paths gradually shifts from black (dark) at the start to yellow (bright) at the end.

with eigenvalues and eigenvectors

$$\lambda_\pm = \pm\frac{1}{2}\hbar\omega,$$

$$|\kappa_\pm\rangle = \sqrt{\frac{\cos^2\theta_1\cos^2\phi + \sin^2\phi}{2 \mp 2\sin\theta_1\cos\phi}}$$
$$\times\left[|0\rangle + \frac{\mp 1 + \sin\theta_1\cos\phi}{\cos\theta_1\cos\phi + i\sin\phi}|1\rangle\right]. \qquad (15)$$

The time evolution operator of the second rotation is

$$U_2(t,t_1) = e^{-\frac{i}{2}\omega(t-t_1)}|\kappa_+\rangle\langle\kappa_+| + e^{\frac{i}{2}\omega(t-t_1)}|\kappa_-\rangle\langle\kappa_-|, \quad (16)$$

which rotates the qubit an additional angle $\theta_2 = \omega(\tau - t_1)$. This rotation is the geodesic path connecting $\mathbf{r}_1$ and $\mathbf{r}_2$ in the lower panel of Fig. 1. The time evolution during the full time

interval $[0, \tau]$ can be written as

$$U(t,0) = \begin{cases} U_1(t,0), & 0 \leqslant t \leqslant t_1, \\ U_2(t,t_1)U_1(t_1,0), & t_1 \leqslant t \leqslant \tau, \end{cases} \tag{17}$$

with the gate $U(\tau,0) = U_2(\tau,t_1)U_1(t_1,0)$ being characterized by the angles θ_1, θ_2, and ϕ, i.e., $U(\tau,0) \equiv \mathbb{U}(\theta_1, \theta_2, \phi)$.

By inserting Eqs. (12) and (16) into Eq. (17), we find the eigenvalues and eigenvectors of $\mathbb{U}(\theta_1, \theta_2, \phi)$:

$$\lambda_\pm = \cos\left(\frac{\theta_1}{2}\right)\cos\left(\frac{\theta_2}{2}\right) - \sin\left(\frac{\theta_1}{2}\right)\sin\left(\frac{\theta_2}{2}\right)\sin\phi \pm i\sqrt{1 - \left[\cos\left(\frac{\theta_1}{2}\right)\cos\left(\frac{\theta_2}{2}\right) - \sin\left(\frac{\theta_1}{2}\right)\sin\left(\frac{\theta_2}{2}\right)\sin\phi\right]^2},$$

$$|\psi_\pm\rangle = \mathcal{N}_\pm\left\{|0\rangle + \frac{\sin\left(\frac{\theta_1}{2}\right)\sin\left(\frac{\theta_2}{2}\right)\cos\phi \pm \sqrt{1 - \left[\cos\left(\frac{\theta_1}{2}\right)\cos\left(\frac{\theta_2}{2}\right) - \sin\left(\frac{\theta_1}{2}\right)\sin\left(\frac{\theta_2}{2}\right)\sin\phi\right]^2}}{e^{i\phi}\cos\left(\frac{\theta_1}{2}\right)\sin\left(\frac{\theta_2}{2}\right) + i\sin\left(\frac{\theta_1}{2}\right)\cos\left(\frac{\theta_2}{2}\right)}|1\rangle\right\}, \tag{18}$$

with normalization factors

$$\frac{1}{\mathcal{N}_\pm} = \sqrt{1 + \frac{2\left(\sin\left(\frac{\theta_1}{2}\right)\sin\left(\frac{\theta_2}{2}\right)\cos\phi \pm \sqrt{1 - \left[\cos\left(\frac{\theta_1}{2}\right)\cos\left(\frac{\theta_2}{2}\right) - \sin\left(\frac{\theta_1}{2}\right)\sin\left(\frac{\theta_2}{2}\right)\sin\phi\right]^2}\right)^2}{1 - \cos\theta_1\cos\theta_2 + \sin\theta_1\sin\theta_2\sin\phi}}. \tag{19}$$

Next, we find the dynamical phases of the evolution by using Eq. (4), yielding

$$\delta_\pm = -\frac{1}{\hbar}\int_0^{t_1}\langle\psi_\pm|H_1|\psi_\pm\rangle dt - \frac{1}{\hbar}\int_{t_1}^\tau\langle\psi_\pm|U_1^\dagger(t_1,0)H_2U_1(t_1,0)|\psi_\pm\rangle dt, \tag{20}$$

where we have taken into account that H_1 and H_2 commute with U_1 and U_2, respectively. Explicitly,

$$U_1^\dagger(t_1,0)H_2U_1(t_1,0) = \frac{\hbar\omega}{2}(-\cos\phi\,\sigma_x + \sin\phi\,\sigma_y). \tag{21}$$

This shows that both integrands on the right-hand side of Eq. (20) are time-independent, which implies

$$\delta_\pm = -\frac{\theta_1}{2}\langle\psi_\pm|\sigma_y|\psi_\pm\rangle - \frac{\theta_2}{2}\langle\psi_\pm|(-\cos\phi\,\sigma_x + \sin\phi\,\sigma_y)|\psi_\pm\rangle = \pm\delta. \tag{22}$$

To find geometric gates, we need to solve for which choices of θ_1, θ_2, and ϕ the dynamical phases become trivial, i.e., satisfy the condition $2\delta = 0, \mod 2\pi$. We thus look for numerical solutions of

$$\theta_1\langle\psi_\pm|\sigma_y|\psi_\pm\rangle + \theta_2\langle\psi_\pm|(-\cos\phi\,\sigma_x + \sin\phi\,\sigma_y)|\psi_\pm\rangle = 0, \mod 2\pi. \tag{23}$$

We restrict to $2\delta = 0$ in the following.

It is possible to find any number of roots for the same set of $\{\theta_1, \phi\}$. In Fig. 2, the roots are shown for when $0 < \theta_1 < 2\pi$ and $0 < \theta_2 < 3\pi$ as functions of ϕ. A positive θ_1 (θ_2) corresponds to a clockwise rotation driven by the first (second) pulse. Roots can be found for counterclockwise rotations to have the same shape but reflected or inverted. For $\theta_1 > 0$, $\theta_2 < 0$, the roots are inverted through the point $(\phi, \theta_2) = (\pi, 0)$; for $\theta_1 < 0, \theta_2 > 0$, on the other hand, they are reflected in the line $\phi = \pi$. When both rotations are counterclockwise the roots are reflected in the line $\theta_1 = 0$. In Fig. 3, the GPs corresponding to these roots are shown. For both counterclockwise rotations where $\theta_1 > 0, \theta_2 < 0$ and $\theta_1 < 0, \theta_2 > 0$ the GPs are reflected in the line $\phi = \pi$ and for the case when both rotations are counterclockwise the GPs are the same as in Fig. 3.

In the upper panel of Fig. 2, one can see that there are three different choices of θ_2 that give a trivial dynamical phase for $\theta_1 = 0.9\pi$. They can be found in narrow ϕ intervals near $\phi \sim 1.15\pi$ and $\phi \sim 1.85\pi$, in between the two sets of dashed lines in the figure. As can be seen in the upper panel of Fig. 3, these choices correspond to different GPs and would thus result in different GNGGs. Furthermore, the width of

the ϕ intervals increases when θ_1 approaches π, until the curve splits into two for $\theta_1 = \pi$, where the first rotation flips the computational states $|0\rangle$ and $|1\rangle$: one concave curve with minimum at $(\phi, \theta_2) = (1.5\pi, \pi)$ (truncated at $\theta_2 = 3\pi$) and one horizontal line at $\theta_2 = \pi$ that corresponds to an "orange slice" shaped loop [39,40]. This loop is the special case where the computational basis and the eigenbasis coincide. In this cyclic case, the GP will be a linear function of the opening angle ϕ [41], which is indeed visible as straight lines in Fig. 3.

One motivating aspect of noncyclic geometric schemes is that they may shorten the exposure to decoherence effects by shortening the run time of the gates. To test this in the two-pulse realization of GNGGs, we use the total precession angle $\theta_1 + \theta_2$ as a natural measure of run time. A closer inspection of Fig. 2 entails that this angle is at least 2π for all roots. It thus appears that the run time cannot be shortened in the two-pulse noncyclic scheme, as compared to cyclic geometric gates with the pulse pair driving the computational basis states along the "orange slice" shaped loops on the Bloch sphere [39,40].

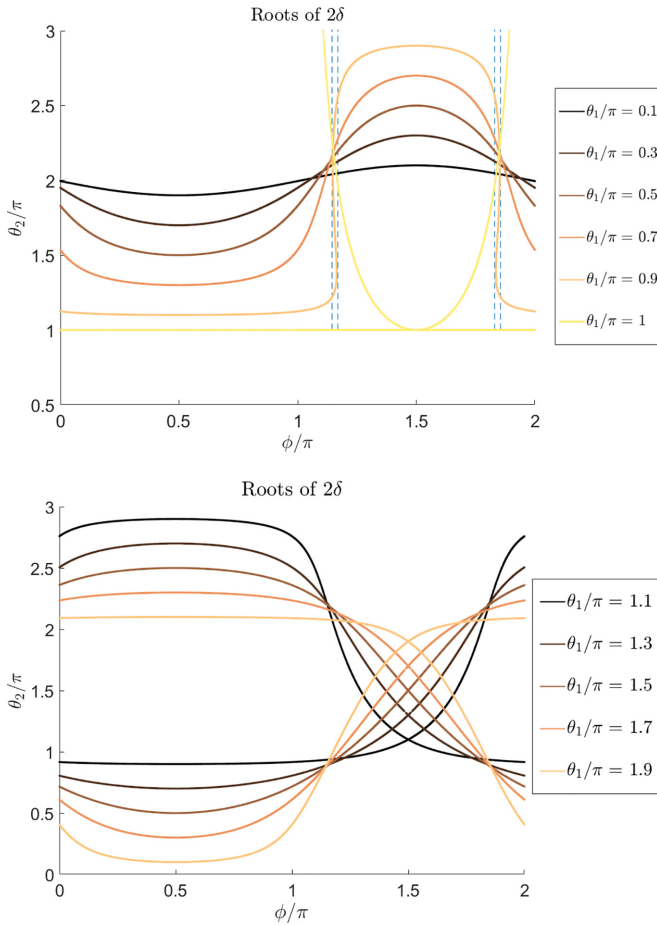To implement a specific gate, both eigenvalues and eigenvectors must match the desired gate. We show that it is

FIG. 2. The roots of $2\delta = 0$ (trivial dynamical phase). θ_1 (θ_2) is the first (second) rotation angle, and ϕ is the angle determining the axis of rotation for the second rotation. In the upper panel, two sets of dashed lines are shown, marking where there are three different choices of θ_2 that give zero dynamical phase for $\theta_1/\pi = 0.9$. The width of these intervals increases when $\theta_1/\pi \to 1$, until the curve splits into two for $\theta_1 = \pi$: one concave curve with minimum at $\phi/\pi = 1.5$ and one horizontal line at $\theta_2/\pi = 1$, the latter corresponding to the special case of cyclic geometric gates.

FIG. 3. GP corresponding to the roots of $2\delta = 0$. θ_1 (θ_2) is the first (second) rotation angle and ϕ is the angle determining the axis of rotation for the second rotation.

IV. CONCLUSION

We proposed a notion of noncyclic geometric gates in which both the computational basis and the eigenbasis acquire purely geometric phases. These two conditions require as precise control of pulse lengths as in the case of cyclic geometric gates, where cyclic evolution of the computational

possible to find any eigenvalue but it is also necessary to find the corresponding eigenvectors. To demonstrate this, eigenvectors corresponding to $2\gamma = \pi$ are displayed in Fig. 4. These eigenvectors cover the entire z axis. Keep in mind that only a first rotation around the y axis has been considered so far. GNGGs with the same eigenvalue and an eigenvector only differing by a rotation around the z axis can be found by changing the first axis of rotation to another in the xy plane, while keeping the relation between the first and the second axis. With this finding any GNGGs with eigenvalue $2\gamma = \pi$, such as the Hadamard gate $\mathbb{H}$, can be realized with only two pulses and it can similarly be shown for other γ as well.

To give an example, we show how a Hadamard gate can be implemented. For this, $2\gamma = \pi$ and eigenvectors correspond to $\pm\frac{\mathbf{e}_x + \mathbf{e}_z}{\sqrt{2}}$ on the Bloch sphere. These eigenvectors are not present in Fig. 4, but can be found by a suitable rotation around the z axis. Figure 5 illustrates this Hadamard gate acting on the computational state $|0\rangle$ and one of the eigenstates.
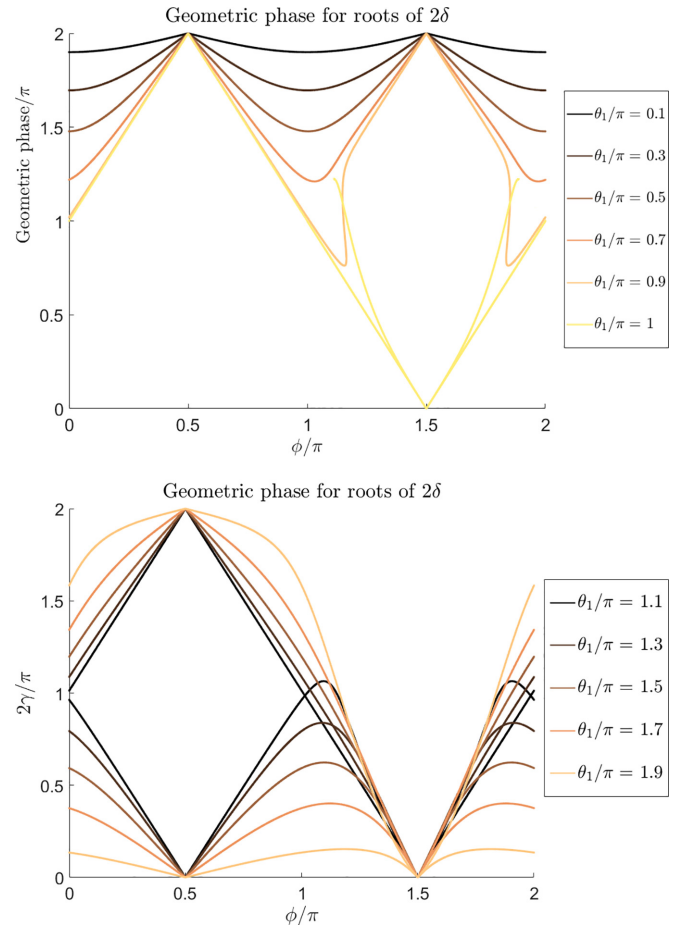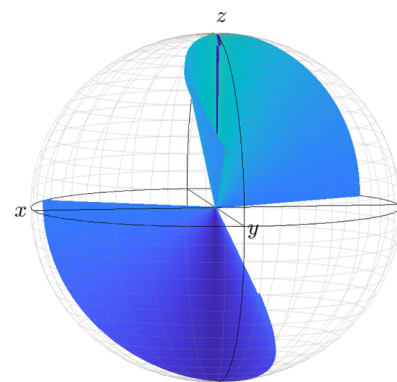

FIG. 4. Continuous set of eigenvectors of gates with $2\gamma = \pi$ with the first rotation taken around the y axis. The eigenvectors are swept so as to form surfaces inside the Bloch sphere of the qubit.
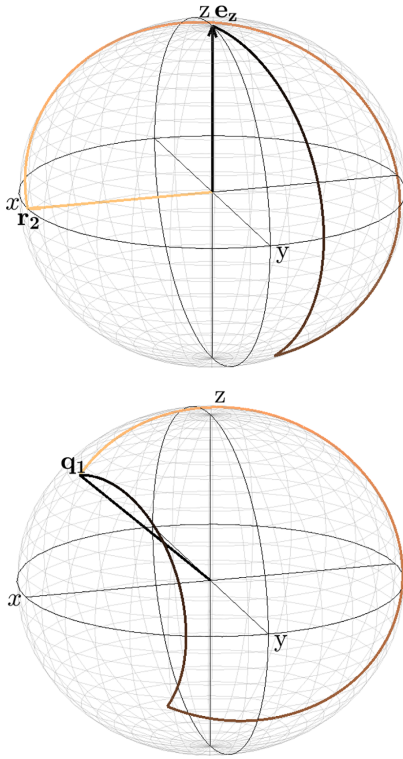
FIG. 5. The path of the $|0\rangle$ state (upper panel) and one of the eigenstates (lower panel) when acted upon by a geometric Hadamard gate. The paths gradually shift from black (dark) at the start to yellow (bright) at the end. The computational state evolves along geodesic segments.

states needs to be ensured. We demonstrated a physical realization of such *genuinely noncyclic geometric gates* in the single-qubit case. This is achieved by using pulse pairs that drive the computational states along pairs of geodesic segments on the Bloch sphere, and simultaneously make the dynamical phase difference of the eigenstates vanish. The proposed concept removes the ambiguity of standard noncyclic geometric gates [24–31], in which the computational basis undergoes purely geometric evolution, while the eigenstates generally do not. Our scheme takes advantage of noncyclic geometric phase to achieve universality.

While the analysis focuses on gates using only two pulses, it can straightforwardly be extended to three or more pulses. This may open up for reduction of accumulated rotation angle as well as more elaborate paths of the computational states, so as to reduce the detrimental effect of noise and decoherence. The scheme may further be extended to nongeodesic evolution of the computational basis to further improve the error resilience of the gates. This extension would require the simultaneous removal of the dynamical phase effects of the computational basis and the eigenstates of the gates. While in this work we focused on the single-qubit case, the genuinely noncyclic geometric scheme can be extended to more general gates involving many qubits or even qudits.

[1] S. Debnath, N. M. Linke, C. Figgatt, K. A. Landsman, K. Wright, and C. Monroe, Demonstration of a small programmable quantum computer with atomic qubits, Nature (London) **536**, 63 (2016).

[2] T. F. Watson, S. G. J. Philips, E. Kawakami, D. R. Ward, P. Scarlino, M. Veldhorst, D. E. Savage, M. G. Lagally, M. Friesen, S. N. Coppersmith, M. A. Eriksson, and L. M. K. Vandersypen, A programmable two-qubit quantum processor in silicon, Nature (London) **555**, 633 (2018).

[3] Y. Wu, Y. Wang, X. Qin, X. Rong, and J. Du, A programmable two-qubit solid-state quantum processor under ambient conditions, npj Quantum Inf. **5**, 9 (2019).

[4] T. Roy, S. Hazra, S. Kundu, M. Chand, M. P. Patankar, and R. Vijay, Programmable Superconducting Processor with Native Three-Qubit Gates, Phys. Rev. Appl. **14**, 014072 (2020).

[5] M. A. Nielsen and I. L. Chuang, *Quantum Computation and Quantum Information* (Cambridge University Press, Cambridge, England, 2000), Chap. 10.6.

[6] D. Gottesman, An introduction to quantum error correction and fault-tolerant quantum computation, Proc. Symp. Appl. Math. **68**, 13 (2010).

[7] J. A. Jones, V. Vedral, A. Ekert, and G. Castagnoli, Geometric quantum computation using nuclear magnetic resonance, Nature (London) **403**, 869 (2000).

[8] A. Ekert, M. Ericsson, P. Hayden, H. Inamori, J. A. Jones, D. K. L. Oi, and V. Vedral, Geometric quantum computation, J. Mod. Opt. **47**, 2501 (2000).

[9] W. Xiang-Bin and M. Keiji, Nonadiabatic Conditional Geometric Phase Shift with NMR, Phys. Rev. Lett. **87**, 097901 (2001).

[10] S.-L. Zhu and Z. D. Wang, Implementation of Universal Quantum Gates Based on Nonadiabatic Geometric Phases, Phys. Rev. Lett. **89**, 097902 (2002).

[11] S.-L. Zhu and Z. D. Wang, Unconventional Geometric Quantum Computation, Phys. Rev. Lett. **91**, 187902 (2003).

[12] Z. S. Wang, C. Wu, X.-L. Feng, L. C. Kwek, C. H. Lai, C. H. Oh, and V. Vedral, Nonadiabatic geometric quantum computation, Phys. Rev. A **76**, 044303 (2007).

[13] B.-J. Liu, X.-K. Song, Z.-Y. Xue, X. Wang, and M.-H. Yung, Plug-and-Play Approach to Non-adiabatic Geometric Quantum Gates, Phys. Rev. Lett. **123**, 100501 (2019).

[14] M. V. Berry, Quantal phase factors accompanying adiabatic changes, Proc. R. Soc. London Ser. A **392**, 45 (1984).

[15] Y. Aharonov and J. Anandan, Phase Change During a Cyclic Quantum Evolution, Phys. Rev. Lett. **58**, 1593 (1987).

[16] D. Leibfried, B. DeMarco, V. Meyer, D. Lucas, M. Barrett, J. Britton, W. M. Itano, B. Jelenković, C. Langer, T. Rosenband, and D. J. Wineland, Experimental demonstration of a ro-

bust, high-fidelity geometric two ion-qubit phase gate, Nature (London) **422**, 412 (2003).

[17] S.-L. Zhu and P. Zanardi, Geometric quantum gates that are robust against stochastic control errors, Phys. Rev. A **72**, 020301(R) (2005).

[18] Y. Ota and Y. Kondo, Composite pulses in NMR as nonadiabatic geometric quantum gates, Phys. Rev. A **80**, 024302 (2009).

[19] Y. Kondo and M. Bando, Geometric quantum gates, composite pulses, and Trotter-Suzuki formulas, J. Phys. Soc. Jpn. **80**, 054002 (2011).

[20] T. Ichikawa, M. Bando, Y. Kondo, and M. Nakahara, Geometric aspects of composite pulses, Philos. Trans. R. Soc. A **370**, 4671 (2012).

[21] S. Berger, M. Pechal, A. A. Abdumalikov, Jr., C. Eichler, L. Steffen, A. Fedorov, A. Wallraff, and S. Filipp, Exploring the effect of noise on the Berry phase, Phys. Rev. A **87**, 060303(R) (2013).

[22] C.-Y. Ding, L.-N. Ji, T. Chen, and Z.-Y. Xue, Path-optimized nonadiabatic geometric quantum computation on superconducting qubits, Quantum Sci. Technol. **7**, 015012 (2022).

[23] M.-J. Liang and Z.-Y. Xue, Robust nonadiabatic geometric quantum computation by dynamical correction, Phys. Rev. A **106**, 012603 (2022).

[24] A. Friedenauer and E. Sjöqvist, Noncyclic geometric quantum computation, Phys. Rev. A **67**, 024303 (2003).

[25] M. Ericsson, D. Kult, E. Sjöqvist, and J. Åberg, Nodal free geometric phases: Concept and application to geometric quantum computation, Phys. Lett. A **372**, 596 (2008).

[26] Z. S. Wang, G. Q. Liu, and Y. H. Ji, Noncyclic geometric quantum computation in a nuclear-magnetic-resonance system, Phys. Rev. A **79**, 054301 (2009).

[27] B. Liu, S. Su, and M. Yung, Nonadiabatic noncyclic geometric quantum computation in Rydberg atoms, Phys. Rev. Res. **2**, 043130 (2020).

[28] L.-N. Ji, C.-Y. Ding, T. Chen, and Z.-Y. Xue, Noncyclic geometric quantum gates with smooth paths via invariant-based shortcuts, Adv. Quantum Tech. **4**, 2100019 (2021).

[29] L. Qiu, H. Li, Z. Han, W. Zheng, X. Yang, Y. Dong, S. Song, D. Lana, X. Tana, and Y. Yu, Experimental realization of noncyclic geometric gates with shortcut to adiabaticity in a superconducting circuit, Appl. Phys. Lett. **118**, 254002 (2021).

[30] L. N. Sun, F. Q. Guo, Z. Shan, M. Feng, L. L. Yan, and S. L. Su One-step implementation of Rydberg nonadiabatic noncyclic geometric quantum computation in decoherence-free subspaces, Phys. Rev. A **105**, 062602 (2022).

[31] F.-Q. Guo, X.-Y. Zhu, M.-R. Yun, L.-L. Yan, Y. Zhang, Y. Jia1, and S.-L. Su, Multiple-qubit nonadiabatic noncyclic geometric quantum computation in Rydberg atoms, Europhys. Lett. **137**, 55001 (2022).

[32] J. W. Zhang, L.-L. Yan, J. C. Li, G. Y. Ding, J. T. Bu, L. Chen, S.-L. Su, F. Zhou, and M. Feng, Single-Atom Verification of the Noise-Resilient and Fast Characteristics of Universal Nonadiabatic Noncyclic Geometric Quantum Gates, Phys. Rev. Lett. **127**, 030502 (2021).

[33] J. Samuel and R. Bhandari, General Setting for Berry's Phase, Phys. Rev. Lett. **60**, 2339 (1988).

[34] N. Mukunda and R. Simon, Quantum kinematic approach to the geometric phase. I. General formalism, Ann. Phys. (NY) **228**, 205 (1993).

[35] Note that the chosen phases of the vectors $|A\rangle = \frac{1}{\sqrt{2}}(|1\rangle - |0\rangle)$ and $|B\rangle = |1\rangle$ in the second term are made such that their Pancharatnam relative phase $\arg\langle A|B\rangle$ [36] vanishes. This is to assure that $e^{i\pi}$ is the GP factor given the assumption that $\mathbb{H}$ is a GNGG.

[36] S. Pancharatnam, Generalized theory of interference, and its applications. Part I. Coherent pencils, Proc. Indian Acad. Sci., Sect. A **44**, 247 (1956).

[37] J. J. Sakurai, *Modern Quantum Mechanics*, 2nd ed. (Addison Wesley Longman, Reading, MA, 1993).

[38] To see this, we note that the eigenstates and computational states coincide for cyclic geometric gates, thus resulting in an Abelian subset consisting of phase shift gates $|q\rangle \mapsto e^{i\gamma_q}|q\rangle$, $q = 0, 1$.

[39] M. Tian, Z. W. Barber, J. A. Fischer, and W. R. Babbitt, Geometric manipulation of the quantum states of two-level atoms, Phys. Rev. A **69**, 050301(R) (2004).

[40] J. T. Thomas, M. Lababidi, and M. Z. Tian, Robustness of single-qubit geometric gate against systematic error, Phys. Rev. A **84**, 042335 (2011).

[41] To see this, we note that an "orange slice" loop with opening angle ϕ encloses the solid angle $\Omega = 2\phi$, which implies the cyclic GPs $\Gamma_0 = -\Gamma_1 = -\frac{1}{2}\Omega = -\phi$.